Magnetic susceptibility and electron magnetic resonance study of monovalent potassium doped manganites $Pr_{0.6}Sr_{0.4-x}K_xMnO_3$

R. Thaljaoui[a,b,c], K. Pękała[b], M. Pękała[c], W. Boujelben[a] J. Szydłowska[c] , J.-F. Fagnard[d], P. Vanderbemden[d], A. Cheikhrouhou[a]

(a) Laboratoire de Physique des Matériaux, Faculté des Sciences de Sfax, Université de Sfax, B. P. 1171, 3000 Sfax, Tunisia.
(b) Faculty of Physics, Warsaw University of Technology, Koszykowa 75, 00-662 Warsaw, Poland.
(c) Department of Chemistry, University of Warsaw, Al. Żwirki i Wigury 101, 02-089, Poland.
(d) SUPRATECS, Department of Electrical Engineering and Computer Science (B28), University of Liege, Belgium.

Abstract

The monovalent potassium doped manganites $Pr_{0.6}Sr_{0.4-x}K_xMnO_3$ (x = 0.05 to 0.2) are characterized using the complementary magnetic susceptibility and electron resonance methods. In paramagnetic phase the temperature variations of the inverse magnetic susceptibility and the inverse intensity of resonance signal obey the Curie-Weiss law. A similarity in temperature variation of resonance signal width and the adiabatic polaron conductivity points to the polaron mechanism controlling the resonance linewidth. The low temperature limit of the pure paramagnetic phase is determined from the electron resonance spectra revealing the mixed phase spread down to the Curie temperature.

Introduction

Recently, doped mixed valence manganites with perovskite structure have attracted much attention due to the rich variety of magnetic, electronic and structural phases [1]. The study of these systems confirms the high correlation between various physical properties [2]. The chance for commercial magnetic application of colossal magnetoresistance and magnetocaloric effects [3, 4] invokes deeper study of these systems. Competition between the ferromagnetic double exchange (DE) and antiferromagnetic superexchange (SE), as well as spin lattice interaction, results in the coexistence of inhomogeneous phases [5]. Several theoretical models have been proposed to explore the underlying mechanisms. Zener [6], using the double exchange mechanism (DE), postulated a model to explain the transition to ferromagnetic- metallic phase which proves that the conduction phenomena are related to itinerant Mn d-electron hopping between Mn^{3+} and Mn^{4+} e_g state. However, recent studies confirm that (DE) model alone cannot explain such colossal magnetoresistance effect. On the other hand, such phenomena have been explained using other models, such as Jahn-Teller effect [7], polaronic effect and phase separation [8]. But the true nature of these phenomena is still a subject of intense studies [9].

Apart from a doping by divalent elements, like Ca, Sr, manganites can be successfully doped with monovalent alkaline earth or silver ions. Due to a valence difference between trivalent rare earth and monovalent ions, the larger fraction of Mn^{3+} ions is transformed to the Mn^{4+} ones. Previously we have reported the study of monovalent sodium doped $Pr_{0.6}Sr_{0.4-x}Na_xMnO_3$ (x = 0, 0.05) manganites [10-13]. Several electron resonance studies have been focused on lanthanum based manganites [14-16], whereas the K - doping effect in $Pr_{0.6}Sr_{0.4}MnO_3$ system have not been studied by electron magnetic resonance method. In the present paper we have extended our investigation on the monovalent doped manganites

$Pr_{0.6}Sr_{0.4-x}K_xMnO_3$ (x = 0.05 to 0.2) [17, 18]. It is aimed to study, how the K doping affects the magnetic phase diagram, which may be modified due to changes of the mean A – site radius and Mn^{3+} content. The complementary AC susceptibility and electron magnetic resonance methods are applied, which are helpful to explain magnetic interaction and spin correlation at a microscopic level.

Experimental

The investigated samples of $Pr_{0.6}Sr_{0.4-x}K_xMnO_3$ (x = 0.05, 0.1, 0.15 and 0.2) were prepared by the standard solid state reaction at high temperature. Stoichiometric ratio of Pr_6O_{11}, $SrCO_3$, $K_2CO_3$and MnO_2 (99.9%) was mixed in an agate mortar and then heated in air to 1000°C for 60 hours with intermediate grinding. The obtained mixtures were then pressed into pellets and sintered at 1100°C. The X-ray diffraction patterns reported for x= 0, 0.05 and 0.1 in previous study [17] and for x= 0.15 and 0.2 in ref [18], respectively, confirm that all studied manganites exhibit single phase with orthorhombic structure corresponding to the *Pnma* space group

The AC magnetic susceptibility was measured in a magnetic field of 10 Oe at 1053 Hz. The field cooled (FC) and zero field cooled (ZFC) magnetization measurements were carried out using ppms system in the temperature range 10 to 340 K with a step of 1 K and under an applied magnetic field of 0.01 T. In order to avoid skin effect the electron magnetic resonance spectra were recorded with loose powder of micrometer size in a capillary using a Bruker spectrometer, operating at 9.44 GHz (X-band). Calibration was carefully performed using DPPH standard as described in ref. [10]. Experimental conditions and methods applied to determine parameters from registered spectra were basically the same as described in [10].

Low field magnetic properties

The temperature dependence of the in-phase component of magnetic susceptibility plotted in Fig. 1A, achieves the relatively narrow maximum just below the Curie temperature T_C shifting from 304 K for x = 0.05 down to 271 K for x = 0.2 (Tab. 1). Below this maximum it diminishes monotonically with decreasing temperature. This low temperature suppression of magnetic susceptibility observed commonly in manganites, is explained in various manner. Most often it is ascribed to the raising contribution of antiferromagnetic Mn^{4+}–Mn^{4+} superexchange interaction [2]. Another scenario is related to a loss of long-range ferromagnetic ordering, occurring at the structurally and magnetically disordered surface layer of the nanometer sized grains. A loss of long range ferromagnetic ordering may be also caused by the magnetic anisotropy present in the material, when the separation of ferro- and antiferromagnetic phases is considered [19, 20].

The out-of-phase component of magnetic susceptibility exhibits a maximum located below T_C and slowly diminishes at lower temperatures for all compositions studied (Fig. 1B). The most abrupt decay is observed on the transition to paramagnetic phase at T_C. This behavior shows that power losses are most intense around Curie temperature and spread over the whole temperature interval of ferromagnetic phase.

The above mentioned T_C values are close to those determined from the temperature variation of DC magnetization registered at a magnetic field of 100 Oe with the field cooled (FC) and zero field cooled (ZFC) protocols [18]. Slightly below T_C the FC and ZFC magnetization curves split at the irreversibility temperature T_{IR} which shifts from 298 K for x = 0.05 to 267 K for x = 0.2.

It was most often observed that the Curie temperature of manganites was enhanced with raising A – site radius [21], which corresponds to raising tolerance factor related to the tilting of MnO_6 octahedra. The double exchange interaction, which is mainly controlling magnetic ordering in manganites, is known to be sensitive to the overlap between the Mn and

oxygen orbitals. Thus, the T_C enhancement occurs since the average bond angle and bond length increase with an increasing A-site radius $<r_A>$ [22].

Our observations for nanostructured manganites $Pr_{0.6}Sr_{0.4-x}K_xMnO_3$ showing that T_C diminishes with raising x, are in contrast to above tendency. The A – site radius of the manganites studied increases from 1.232 Å for x = 0.05 to 1.274 Å for x = 0.2 [18] in agreement with tolerance factor varying from 0.954 for x = 0 to 0.977 for x = 0.2. However, this is accompanied by a slight suppression of Curie temperature. Such an opposite tendency may be related to the random disorder of Pr, Sr and K cations with different sizes distributed over the *A* sites in the manganite structure. This cationic size mismatch involves the oxygen displacement may be accounted for by the variance of the A-cation radius distribution which is defined as

$$\sigma^2 = \sum_i y_i r_i^2 - \langle r_A \rangle^2 \qquad (1)$$

where y_i is a fraction if cation i and $\langle r_A \rangle$ is a mean r_A radius. The σ^2 values evolve from 0.0095 for x = 0.05 to 0.0220 for x = 0.2 (Tab. 1) revealing the increasing oxygen disorder, which in turn reduces the orbital overlap. These results in a weakening of double exchange interaction indicated by monotonically reduced T_C values (Fig. 1D). The T_C reduction with raising σ^2 values is an universal feature of manganites reported in ref. [23]. Moreover, strength of double exchange interaction depends additionally on microstructural features being weakened by the structurally and magnetically disordered surface layer of nanostructured grains.

The magnetic susceptibility in paramagnetic phase for each prepared sample was checked to obey the Curie – Weiss law

$$\chi = \frac{C}{T - \theta_S} \qquad (2)$$

where the Curie constant $C = \mu_0 N \mu_{eff}^2$. Only the linear part of the plot of inverse magnetic susceptibility versus temperature was applied since the magnetic susceptibility starts to deviate from Curie-Weiss law below the T_S temperature (Tab. 1), as plotted in Fig. 1C. The fitting to experimental data enables to determine the Weiss temperature θ_S and effective magnetic moment, listed in Tab. 1. Values of effective magnetic moment per formula unit μ_{eff}, calculated assuming the perfect stoichiometry, diminish slowly from 6.16 μ_B for x = 0.05 down to 5.90 μ_B for x = 0 .2. The measured effective magnetic moments are about 5 to 7 % lower than the ideal values calculated taking into account the moments of Pr and Mn ions listed in [24] and corresponding fractions of Mn^{3+} and Mn^{4+} ions. This difference proves that the relative orientation of these ionic moments remains almost parallel. The θ_S parameter varies smoothly from 305 K for x = 0.05 down to 274 K for x = 0.2. Such a behavior confirms that the K doping weakens the effective interaction between magnetic moments in the paramagnetic phase.

Discussion of magnetic results

The registered electron spin resonance spectra of all manganites studied exhibit the maximum amplitude just above the Curie temperatures T_C (Fig. 2), which is characteristic also for Na doped manganites [10, 25]. In the paramagnetic phase the spectra contain a single Lorentzian type signal whereas deviations from this shape start to appear when approaching the ferromagnetic phase. This reveals the local magnetic inhomogeneity or phase separation effects [26]. The asymmetry of resonance signals defined by a ratio of maximum to minimum of signal derivative is almost constant and close to 1 within the 4 % limit in paramagnetic phase (Fig. 3). With decreasing temperature the signal asymmetry raises abruptly about 25 K above T_C, which is due to the overlap with ferromagnetic signal. In the paramagnetic phase

the magnetic resonance field is practically centered about 3338 Oe and drops down, when the ferromagnetic ordering comes into a play (Fig. 4). The g_{eff} values in paramagnetic phase are in a range 2.0115 to 2.0223.

The temperature variation of signal width ΔH_{p-p} (T) of manganites studied (Fig. 5) exhibits a minimum at T_{min} located a few percent above phase transition temperature T_C (Tab. 1). The similar behavior was reported for the Na doped $Pr_{0.6}Sr_{0.4-x}Na_xMnO_3$ manganites [10] and for $Pr_{0.7}Ca_{0.15}Ba_{0.15}MnO_3$ manganites [27- 29]. The ΔH_{p-p} (T) minimum shifts towards lower temperatures with raising K content. At elevated temperatures ΔH_{p-p} (T) grows moderately with temperature. The more sudden enhancement of ΔH_{p-p} (T) is observed when lowering temperature within the ferromagnetic state.

Due to the high sensitivity of resonance technique the measured linewidth ΔH_{p-p} (T), its minimum value as well as its location at T_{min} are strongly dependent on sample quality. An influence of inhomogeneities arising from variations of chemical composition, oxygen stoichiometry or grain sizes was confirmed, e.g. for the $La_{1-x}Sr_xMnO_3$ and $La_{1-x}Ba_xMnO_3$ thin films [30] and single crystals and powder of $La_{0.67}Sr_{0.33}MnO_3$ [28]. In the paramagnetic phase the ΔH_{p-p} (T) of the $La_{0.67}Sr_{0.33}MnO_3$ manganites is only slightly different for the powder and single crystal whereas the pronounced split is observed below Curie temperature. An abrupt jump of ΔH_{p-p} (T) in ferromagnetic phase reported also for polycrystalline $Pr_{0.7}Sr_{0.3}MnO_3$ [31, 32], appears to be characteristic for manganites.

Temperature dependence of signal width ΔH_{p-p}(T) is a puzzling question in manganites and various approaches have been proposed in the past. This question is burdensome since there is no theoretical model for a spin – lattice relaxation in manganites. Generally, a variation of ΔH_{p-p}(T) is compared the temperature dependence of electrical resistivity and/or magnetic susceptibility, in order to confirm or exclude some mechanisms considered. Most often the possible polaron contribution is analyzed. Applying the small polaron model above T_{min} the temperature variation of signal width ΔH_{p-p}(T) was well fitted using the following formula [33]:

$$\Delta H_{P-P}(T) = \Delta H_0 + \left(A/T\right)\exp\left(-E_P/k_BT\right) \qquad (3)$$

where ΔH_0 is a constant and k_B is the Boltzmann constant. The obtained activation energies E_P are equal to 128, 154, 177 and 139 meV, respectively, for x = 0.05 to 0.2. They are comparable with previously reported values [10, 11] but the evolution of activation energy is not monotonous with K- content, which can be related to the variation of angles Mn-O-Mn as described previously [18]. These values are lower than energies E_S derived from magnetic susceptibility. The difference in activation energies may be attributed to different "frequency windows" specific for magnetic resonance and susceptibility techniques. Thus, the last equation being similar to that one describing the adiabatic polaron conductivity [27], seems to be in favor to the polaron mechanism in linewidth dependence in paramagnetic phase.

The signal intensity, determined by using the peak to peak amplitude α and width ΔH_{p-p} according to the following relation: $I(T) = \alpha\ \Delta H_{p-p}^2$, is a monotonically diminishing as a function of temperature both in the ferromagnetic and paramagnetic phases (Fig. 6). The temperature variation of I(T) data can be well described using the following expression [31]:

$$I(T) = I_0 \exp\left(\frac{E_S}{k_BT}\right) \qquad (4)$$

where E_S is the activation energy. The E_S values determined from the spectra are equal to 193, 262, 225 and 276 meV for x varying from 0.05 to 0.2, respectively (Tab. 1).

In the paramagnetic phase the signal intensity is known to be proportional to magnetic susceptibility. The temperature dependence of the inverse intensity was used to check, if the Curie – Weiss law is obeyed in paramagnetic phase (Fig. 7).

$$I(T) \propto \frac{C}{T - \theta_I} \tag{5}$$

where θ_I is a Weiss temperature and C is a Curie constant. The derived values of Weiss parameter θ_I, derived from inverse signal intensity, vary from 305 K for x = 0.05 to 274 K for x = 0.2 sample (Tab. 1). Such positive values of θ_I reveal the prevailing relatively strong ferromagnetic interaction between magnetic moments [18]. It is worth to notice, that deviations from a Curie – Weiss law applied to signal intensity, start to appear below the T_I temperature, more than 10 K above the Weiss temperature θ_I.

The information collected from experimental data are summarized in the magnetic phase diagram of the manganites studied (Fig. 8). The plotted ferromagnetic Curie temperatures T_C determined from a minimum in temperature derivative of magnetic susceptibility lie on the lowest curve. The medium curve corresponds to temperatures T_S, below which inverse magnetic susceptibility starts to deviate from Curie-Weiss law. The upper curve shows temperatures T_I at which inverse resonance intensity starts to deviate from Curie-Weiss law. A simple interpretation of this phase diagram reminds that in the ideal case above the Curie temperature T_C the spontaneous magnetization disappears. However, the ferromagnetic ordering may survive even above T_C due to the materials inhomogeneity and the external magnetic field. This surviving magnetization is revealed by deviations from Curie-Weiss law applied to susceptibility, as seen below T_S which are located, for a few K, above T_C. The electron magnetic resonance, known to be the more sensitive probe than magnetic susceptibility, detects very early stages of ferromagnetic ordering up to the higher temperature T_I. Thus, one may conclude that the T_I curve determines the low temperature limit of pure paramagnetic phase, whereas some kind of mixed phase exists between the T_C and T_I curves. A nature of the mixed phase is different from the so called Griffiths phase since the manganites studied do not exhibit the downturn deviation in magnetic susceptibility nor inverse intensity of signal [34]. There is also no indication of Griffiths phase in resonance signal registered for manganites studied [35]. In contrast to the Griffiths phase containing relatively large ferromagnetic clusters, the observed mixed phase seems to be built of small clusters.

Conclusions

Despite of the raising mean A – site radius, the Curie temperature T_C is reduced for higher potassium doping fraction varying from 0.05 to 0.2, which is caused by the raising variance of the A-cation radius distribution, which is an universal feature of manganites [23]. A similarity in temperature variation of resonance signal width and the adiabatic polaron conductivity points to the polaron mechanism responsible for the resonance linewidth. The complementary investigation of monovalent K doped manganites by means of magnetic susceptibility and electron resonance reveals a presence of local ferromagnetic correlations in the mixed phase spreading in a phase diagram between the ferromagnetic Curie and T_I temperatures. No traces of the so called Griffiths phase are detected. The presented combined method employing the magnetic susceptibility and electron magnetic resonance methods may be also applicable to a deeper characterization of other materials.

Acknowledgements. This work performed within the COST MP903 action was supported in parts by the Tunisian Ministry of Higher Education and Scientific Research, Ministry of Science and Higher Education (PL) and WBI (B) in a frame of scientific exchange agreement.

References

[1] Colossal Magnetoresistance Oxides, edited by Y. Tokura (Gordon and Breach, New York, 2000)
[2] A.M. Haghiri-Gosnet, J.-P. Renard, J. Phys. D: Appl. Phys. 36 (2003) R127.
[3] C. N. R. Rao, B. Raveau (Eds.), Colossal Magnetoresistance, Charge Ordering and Related Properties of Manganese Oxides, World Scientific, Singapore, 1998.
[4] A. M. Tishin, Y. I. Spichkin, The Magnetocaloric Effect and Its Applications, Institute of Physics, Bristol, 2003.
[5] E. Dagotto, Nanoscale Phase Separation and Colossal Magnetoresistance, Springer Series in Solid State Physics Vol. 136 (Springer-Verlag, Berlin, Heidelberg, 2003).
[6] C. Zener, Phys. Rev. 82, 403 (1951).
[7] E. Pollert, S. Krupicka, E. Kuzmicova, J. Phys. Chem. Solids 43 (1982) 1137
[8] S. Mori, C. H. Chen, S. W. Cheong, Phys. Rev. Lett. 81(1998) 3972.
[9] H.-Y. Hwang, S.-W. Cheong, P. G. Radaelli, M. Marezio, B. Batlogg, Phys. Rev. Lett. 75 (1995) 914.
[10] R. Thaljaoui, W. Boujelben, M. Pękała, J. Szydłowska, A. Cheikhrouhou, J. Alloys Compds 526 (2012) 98
[11] R. Thaljaoui, W. Boujelben, M. Pękała, D. Pociecha, J. Szydłowska, A. Cheikhrouhou, J. Alloys Compds 530 (2012) 138
[12] R. Thaljaoui, W. Boujelben, M. Pękała, K. Pękała, J. Mucha, A. Cheikhrouhou, J. Alloys Compds 558 (2013) 236
[13] R. Thaljaoui, W. Boujelben, M. Pękała, K. Pękała, W. Cheikhrouhou-Koubaa, A. Cheikhrouhou, J. Mater Sci 48 (2013) 3894
[14] T.L. Phan, N.D. Tho, L.V. Bau, N.X. Phuc, S.C. Yu, J. Mag. Mag. Materials 303 (2006) e339–e341.
[15] D. L. Huber, G. Alejandro, A. Caneiro, M. T. Causa, F. Prado, and M. Tovar, S. B. Oseroff, Phys. Rev. B 60, 12155 (1999).
[16] A. Shengelaya, Guo-meng Zhao, H. Keller, and K. A. Müller, Phys. Rev. Lett. 77 (1996) 5296.
[17] R. Thaljaoui, W. Boujelben, M. Pękała, A. Cheikhrouhou, J. Supercond Nov Magn 26 (2013) 1625
[18] R. Thaljaoui, W. Boujelben, M. Pękała, K. Pękała, J.-F. Fagnard, P. Vanderbemden, M. Donten. A. Cheikhrouhou. (Submitted to Journal of Magnetism and Magnetic Materials).
[19] S. Ravi, Manoranjan Kar, Physica B 348 (2004) 169
[20] S. Roeßler, Harikrishnan S. Nair, U. K. Roeßler, C. M. N. Kumar, Suja Elizabeth, and S. Wirth, Phys. Rev B 84 (2011) 184422
[21] J. M. D. Coey, M. Viret, S. von Molnar, Advances in Physics, 48 1999 167
[22] K. Doerr, J. Phys. D: Appl. Phys. **39** (2006) R125
[23] L. M. Rodriguez-Martinez, J. P. Attfield; Phys. Rev. B 54, 15622 (1996).
[24] JMD Coey, Magnetism and Magnetic Materials, Cambridge Un. Presss 2010.
[25] R. Thaljaoui, W. Boujelben, M. Pekała, J. Szydłowska and A. Cheikhrouhou, EPJ Web of Conf, 29 (2012) 00050.
[26] J. Yang, X. Rong, D. Suter, Y. P. Sun, Phys. Chem. Chem. Phys., 13 (2011) 16343
[27] A.N. Ulyanov, H.D.Quang , N.E.Pismenova , S.C.Yu , G.G.Levchenko Solid State Communications 152 (2012) 1556
[28] M.T. Causa M. Tovar, A. Caneiro, F. Prado, G. Ibanez, C. A. Ramos, A. Butera, B. Alascio, X. Obradors, S. Pinol, F. Rivadulla, C. Vazquez-Vazquez, M. A. Lopez-Quintela, J. Rivas, Y. Tokura, S. B. Oseroff, Phys. Rev. B 58 (1998) 3233

[29] C. Rettori, D. Rao, J. Singley, D. Kidwell, S. B. Oseroff, M. T. Causa, J. J. Neumeier and K. J. McClellan, S-W. Cheong, S. Schultz, Phys. Rev. B 55 (1997) 3083
[30] R. Bah, D. Bitok, R. R. Rakhimov, M. M. Noginov, A. K. Pradhan, and N. Noginova, J. of Applied Physics 99 (2006) 08Q312
[31] P.H. Quang, Y.S. Chung, A.N. Ulyanov, N.E. Pismenova, S.C. Yu, Phys. Stat. Sol. B 241 (2004) 1569
[32] N. Rama, K. Mohan Kant, V. Sankaranarayanan, M.S. Ramachandra Rao, Journal of Magnetism and Magnetic Materials 303 (2006) e342–e346
[33] A. Shengelaya, G.M. Zhao, H. Keller, K.A. Muller, B.I. Kochelaev, Phys. Rev. B 61 (2000) 5888
[34] G Narsinga Rao, J W Chen, S Neeleshwar, Y Y Chen and MK Wu, J. Phys. D: Appl. Phys. 42 (2009) 095003
[35] S.I. Andronenko, A.A. Rodionov, A.V. Fedorova, S.K. Misra, J. Magn. Magne. Materials 326 (2013) 151

Figures

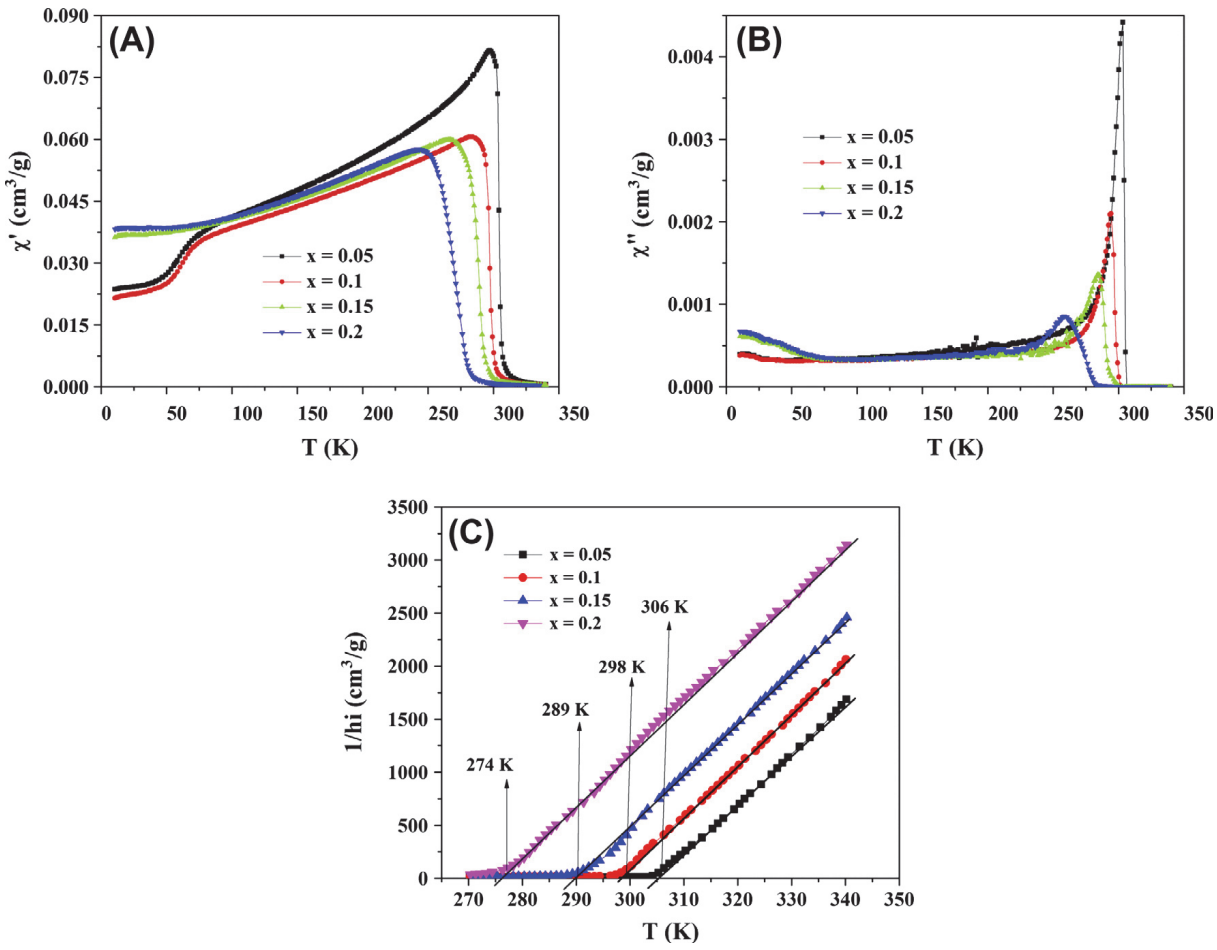

Fig. 1A-C. Temperature variation of in-phase (A) and out-of-phase (B) components of AC magnetic susceptibility and the inverse susceptibility (C) of manganites $Pr_{0.6}Sr_{0.4-x}K_xMnO_3$ (x = 0.05, 0.1, 0.15 and 0.2).

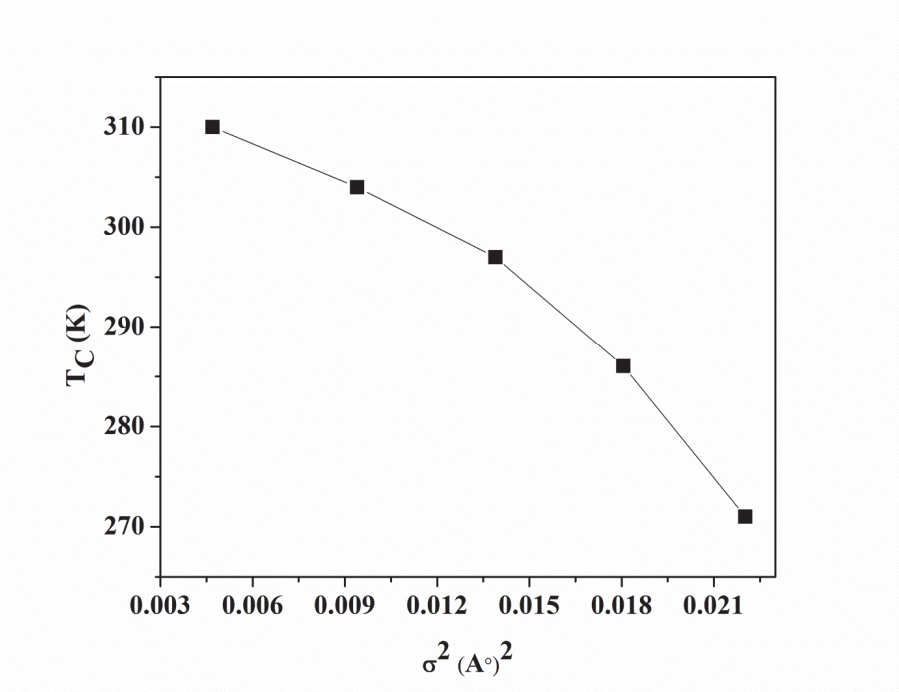

Fig. 1D. The Curie temperature as a function of the variance of the A-cation radius distribution (equation 1).

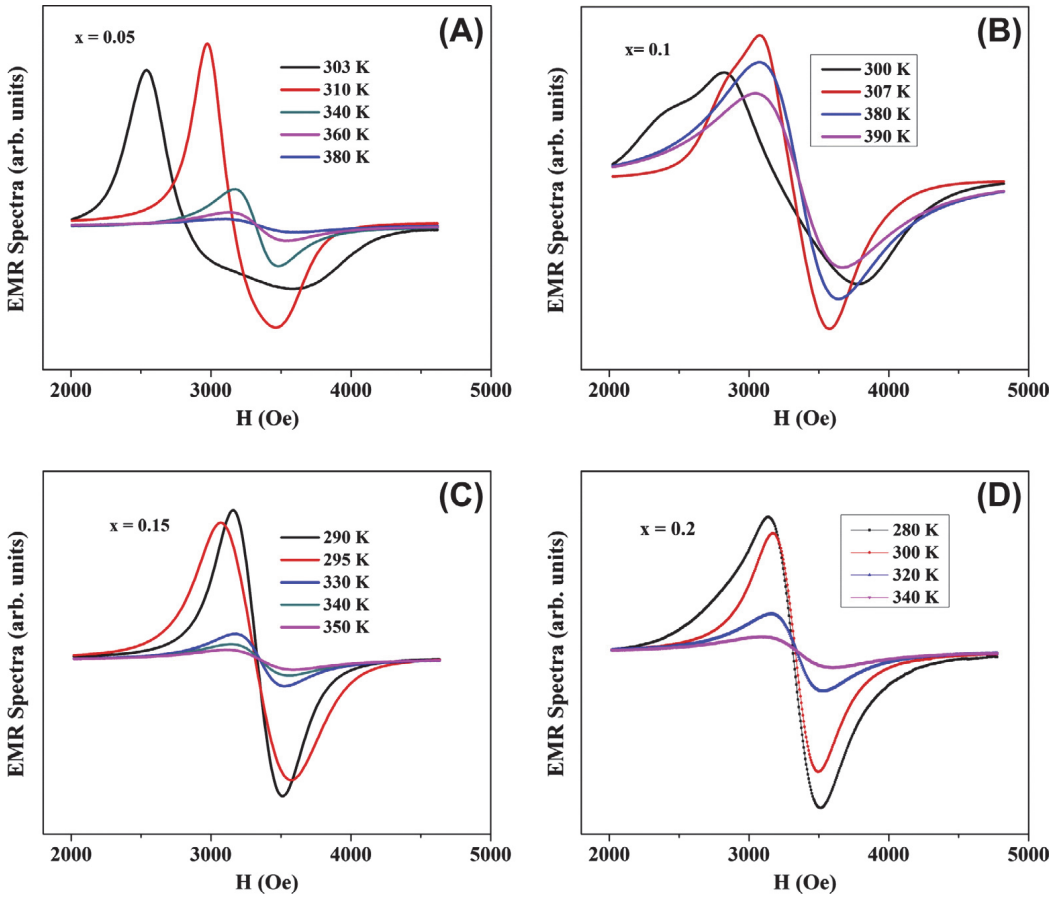

Fig. 2A-D. Selected electron magnetic resonance spectra of manganites $Pr_{0.6}Sr_{0.4-x}K_xMnO_3$ (x = 0.05, 0.1, 0.15 and 0.2).

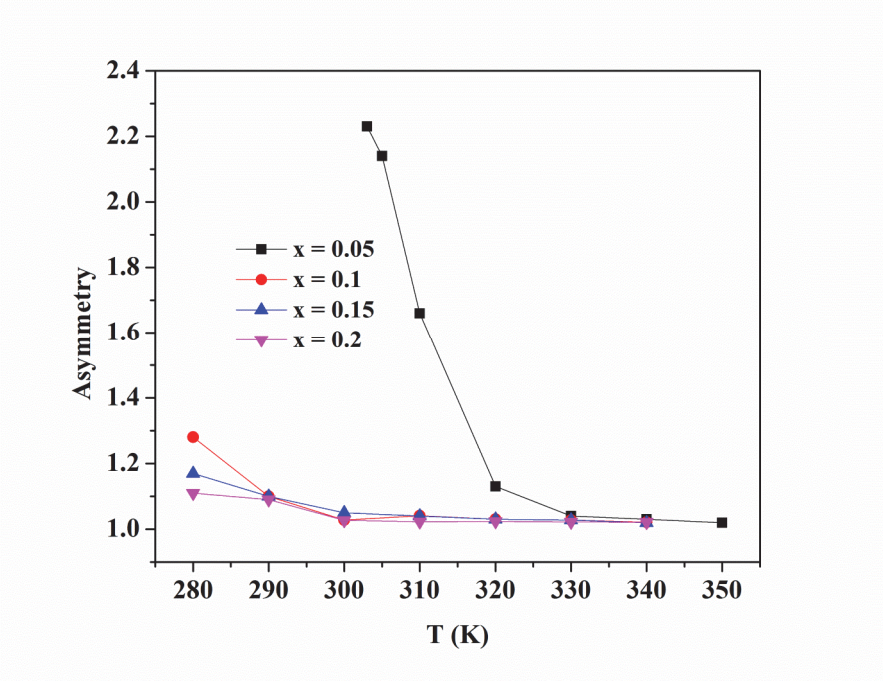

Fig. 3. Temperature variation of signal asymmetry of manganites $Pr_{0.6}Sr_{0.4-x}K_xMnO_3$ (x = 0.05, 0.1, 0.15 and 0.2).

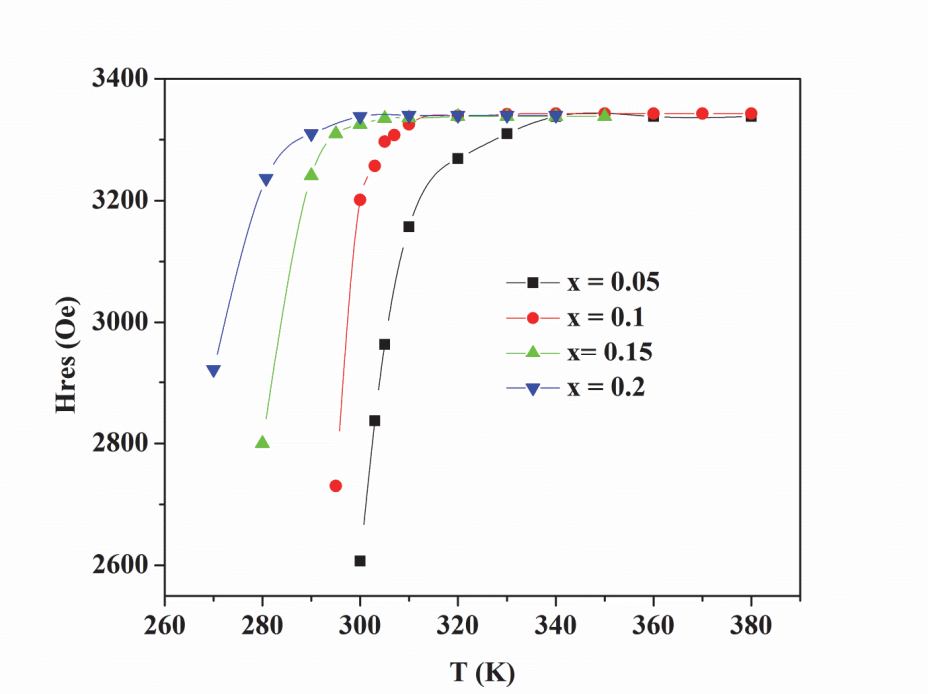

Fig. 4. Temperature variation of magnetic resonance field of manganites $Pr_{0.6}Sr_{0.4-x}K_xMnO_3$ (x = 0.05, 0.1, 0.15 and 0.2).

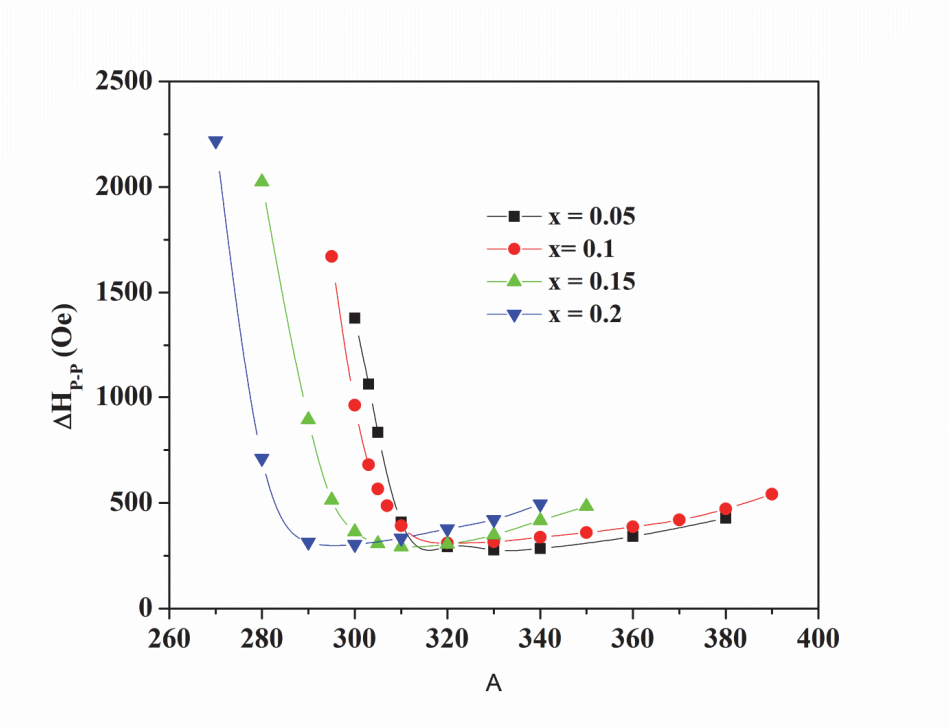

Fig. 5. Temperature variation of peak to peak linewidth of manganites $Pr_{0.6}Sr_{0.4-x}K_xMnO_3$ (x = 0.05, 0.1, 0.15 and 0.2).

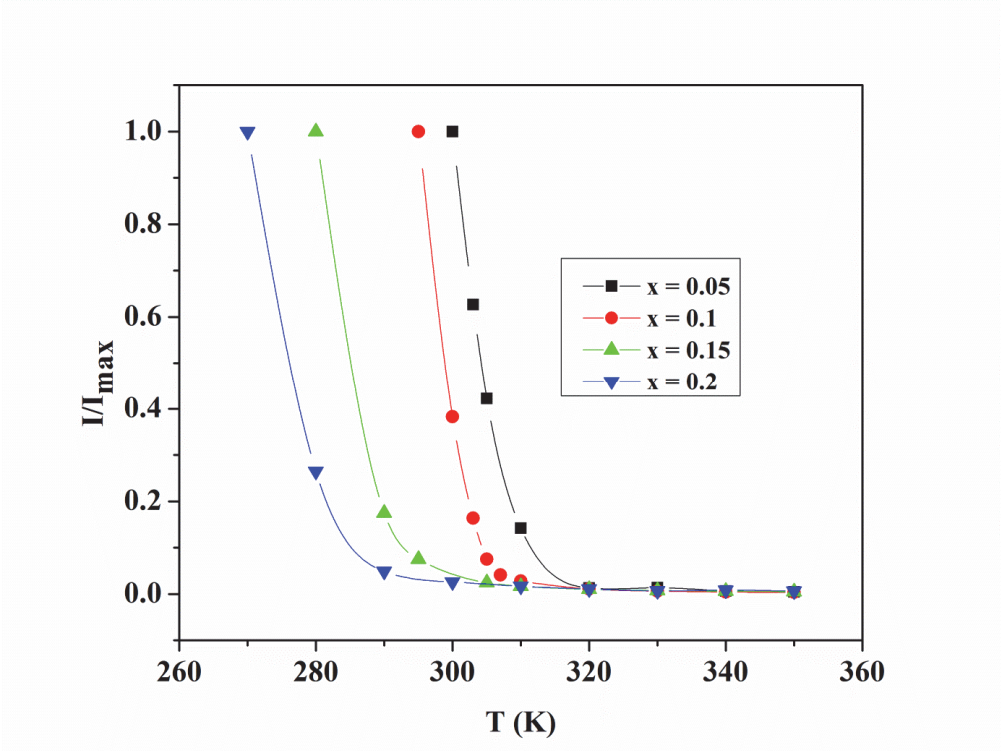

Fig. 6. Temperature variation of signal intensity of manganites $Pr_{0.6}Sr_{0.4-x}K_xMnO_3$ (x = 0.05, 0.1, 0.15 and 0.2).

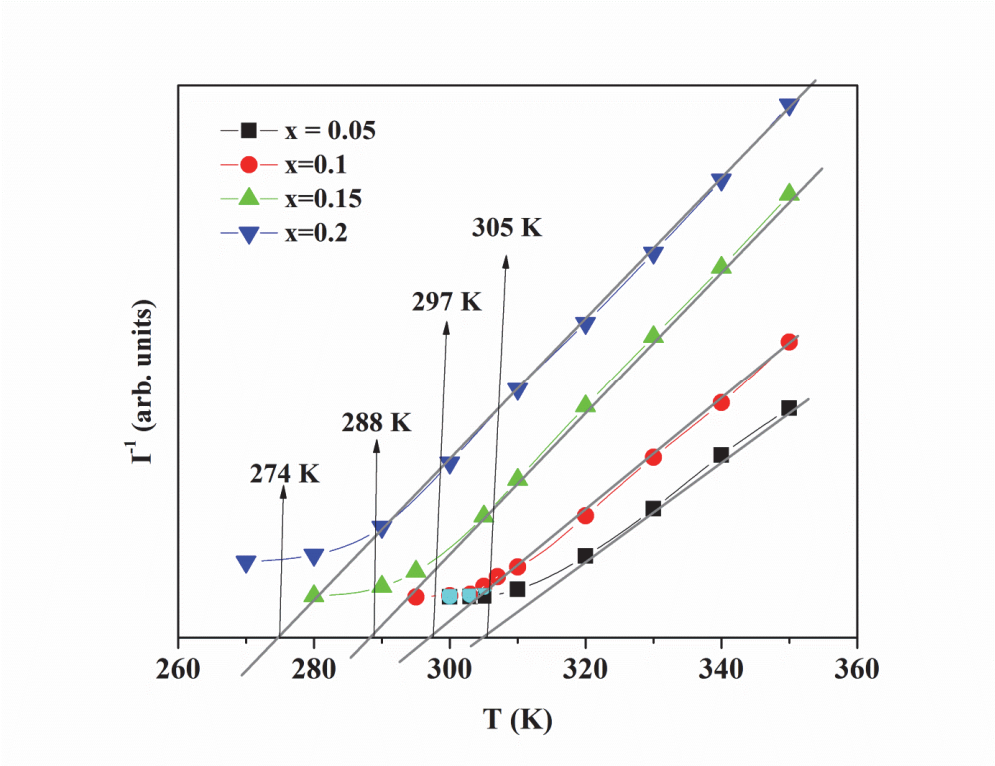

Fig. 7. Temperature variation of inverse signal intensity of manganites $Pr_{0.6}Sr_{0.4-x}K_xMnO_3$ (x = 0.05, 0.1, 0.15 and 0.2).

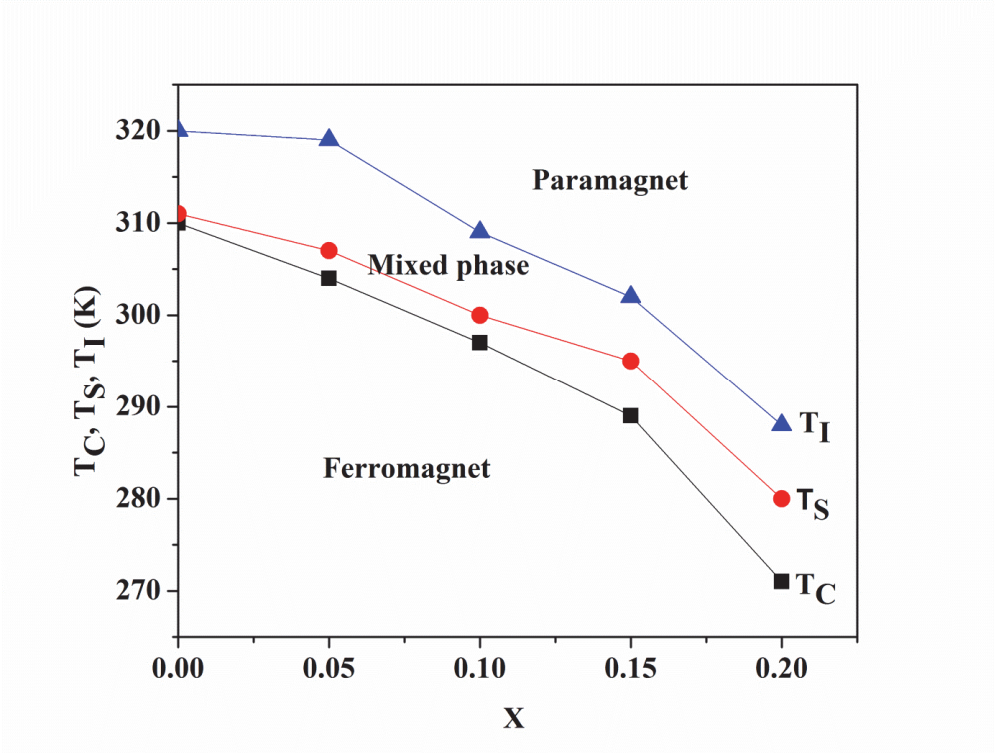

Fig. 8. Phase diagram of manganites $Pr_{0.6}Sr_{0.4-x}K_xMnO_3$ showing the Curie temperature T_C, temperature T_S at which inverse susceptibility starts to deviate from Curie-Weiss law and temperature T_I at which inverse resonance intensity starts to deviate from Curie-Weiss law.

Table 1. Experimental parameters for manganites $Pr_{0.6}Sr_{0.4-x}K_xMnO_3$ (x = 0.05, 0.1, 0.15 and 0.2).

x	0.05	0.1	0.15	0.2
Mn^{3+}(%)	55	50	45	40
$\langle r_A \rangle$ (Å)	1.24	1.25	1.26	1.27
σ^2 (Å^2)	0.0087	0.0130	0.0171	0.0501
T_C (K)	304	297	289	271
T_{IR} (K)	298	289	280	267
T_S (K)	308	300	295	280
μ_{eff} (μ_B)	6.16	6.04	5.92	5.90
θ_S (K)	306	298	289	274
T_{min} (K)	330	320	310	300
T_I (K)	319	309	302	278
θ_I (K)	305	297	288	274
E_S (meV)	193	262	225	276
E_P (meV)	128	154	177	139